Protein Science (1997), *6*:1734–1745. Cambridge University Press. Printed in the USA.

Heteronuclear NMR assignments and secondary structure of the coiled coil trimerization domain from cartilage matrix protein in oxidized and reduced forms

RONALD WILTSCHECK,[1] RICHARD A. KAMMERER,[2] SONJA A. DAMES,[1] THERESE SCHULTHESS,[2] MARCEL J.J. BLOMMERS,[3] JÜRGEN ENGEL,[2] AND ANDREI T. ALEXANDRESCU[1]

[1]Department of Structural Biology, Biozentrum, University of Basel, Basel, Switzerland, CH-4056
[2]Department of Biophysical Chemistry, Biozentrum, University of Basel, Basel, Switzerland, CH-4056
[3]Novartis Pharma AG, Basel, CH-4002, Switzerland

(RECEIVED March 5, 1997; ACCEPTED April 30, 1997)

Abstract

The C-terminal oligomerization domain of chicken cartilage matrix protein is a trimeric coiled coil comprised of three identical 43-residue chains. NMR spectra of the protein show equivalent magnetic environments for each monomer, indicating a parallel coiled coil structure with complete threefold symmetry. Sequence-specific assignments for ^{1}H-, ^{15}N-, and ^{13}C-NMR resonances have been obtained from 2D ^{1}H NOESY and TOCSY spectra, and from 3D HNCA, ^{15}N NOESY-HSQC, and HCCH-TOCSY spectra. A stretch of α-helix encompassing five heptad repeats (35 residues) has been identified from intra-chain HN-HN and HN-Hα NOE connectivities, $^{3}J_{\mathrm{HNH}\alpha}$ coupling constants, and chemical shift indices. The α-helix begins immediately downstream of inter-chain disulfide bonds between residues Cys 5 and Cys 7, and extends to near the C-terminus of the molecule. The threefold symmetry of the molecule is maintained when the inter-chain disulfide bonds that flank the N-terminus of the coiled coil are reduced. Residues Ile 21 through Glu 36 show conserved chemical shifts and NOE connectivities, as well as strong protection from solvent exchange in the oxidized and reduced forms of the protein. By contrast, residues Ile 10 through Val 17 show pronounced chemical shift differences between the oxidized and reduced protein. Strong chemical exchange NOEs between HN resonances and water indicate solvent exchange on time scales faster than 10 s, and suggests a dynamic fraying of the N-terminus of the coiled coil upon reduction of the disulfide bonds. Possible roles for the disulfide crosslinks of the oligomerization domain in the function of cartilage matrix protein are proposed.

Keywords: α-helix; coiled coil; disulfide bonds; flexibility; heteronuclear NMR; hydrogen exchange; oligomerization domain

The α-helical coiled coil is a common protein structural motif. Examples of coiled coils are found in extracellular proteins, muscle proteins, cytoskeletal components, viral surface proteins, transcription factors, and tumor suppressors (Lupas, 1996). In many of these proteins coiled coil domains mediate oligomerization (Lupas, 1996; Kammerer, 1997). There is a great diversity of coiled coils, with oligomerization states ranging from dimers to pentamers (Harbury et al., 1993; Malashkevich et al., 1996). A common feature of coiled coils is that their primary sequences share a highly characteristic seven-residue "heptad repeat" $(abcdefg)_n$, with residues *a* and *d* predominantly hydrophobic and with residues *e* and *g* often occupied by charged residues (Hodges et al., 1972; McLachlan & Stewart, 1975; Cohen & Parry, 1990). Because the rules governing the formation of coiled coils are relatively well understood compared to those for globular proteins, there has been substantial progress in identifying coiled coils from amino acid sequence (Parry, 1982; Lupas et al., 1991; Berger et al., 1995), in predicting coiled coil oligomerization states (Harbury et al., 1993; Woolfson & Alber, 1995), and in the design of coiled coils (Betz et al., 1995).

Reprint requests to: Andrei T. Alexandrescu, Department of Structural Biology, Biozentrum, University of Basel, Klingelbergstr. 70, CH-4056 Basel, Switzerland; e-mail: alexandrescu@ubaclu.unibas.ch.

Abbreviations: 2D, two-dimensional; 3D, three-dimensional; ΔG_u, change in free energy on unfolding; CD, circular dichroism; CMP, cartilage matrix protein; CMPcc, coiled coil domain of chicken CMP; DIPSI, decoupling in the presence of scalar interactions; DTT, dithiothreitol; HCCH-TOCSY, ^{1}H-^{13}C HSQC combined with ^{13}C TOCSY; IPTG, isopropyl β-D-thiogalactopyranoside; HNCA, (amide proton)-(nitrogen)-(α-carbon) correlation; HNHA, (amide proton)-(nitrogen)-(α-proton) correlation; HNHB, (amide proton)-(nitrogen)-(β-proton) correlation; HSQC, heteronuclear single-quantum coherence spectroscopy; NEM, *N*-ethyl maleimide; NOE, nuclear Overhauser effect; NOESY, NOE spectroscopy; OD, optical density; P_f, protection factor; PCR, polymerase chain reaction; TOCSY, total correlation spectroscopy; TPPI, time proportional phase incrementation.

Cartilage matrix protein (CMP), also known as matrilin 1 (Deák et al., 1997), is one of the most abundant non-collagenous extracellular proteins of the cartilage matrix. Although the precise function of the protein is unknown, its association with the proteoglycan aggrecan (Paulsson & Heinegård, 1981) and with collagen (Tondravi et al., 1993) suggests that the protein is an integral component of cartilage collagen fibrils (Winterbottom et al., 1992). A possible role for CMP in the regulation of cartilage matrix assembly has been suggested (Hauser & Paulsson, 1994). CMP consists of three identical polypeptide chains (trimer MW 148 kDa). Each chain consists of four domains: domains 1 and 3 show homology to von Willebrand factor type A; domain 2 has homology to epidermal growth factor; domain 4 contains the characteristic heptad repeats of a coiled coil motif (Hauser & Paulsson, 1994).

The 43-residue C-terminal domain (CMPcc) that is the subject of the present study corresponds to residues 451–493 of chicken CMP (Argraves et al., 1987). Residues C7 through K41 span five heptad repeats in the sequence of CMPcc (Fig. 1). Mutagenesis studies indicate that C5 and C7, directly upstream of the heptad repeats form inter-chain disulfide bonds (Haudenschild et al., 1995). These disulfide bonds have been postulated to enhance the stability of the coiled coil structure once formed (Haudenschild et al., 1995; Beck et al., 1996). In this paper we report ^{1}H-, ^{15}N-, and ^{13}C-NMR resonance assignments for CMPcc. Additional results on the NMR characterization of the extent of α-helical secondary structure in CMPcc, and on the role of the interchain disulfide bonds in restricting the flexibility of this structure are presented.

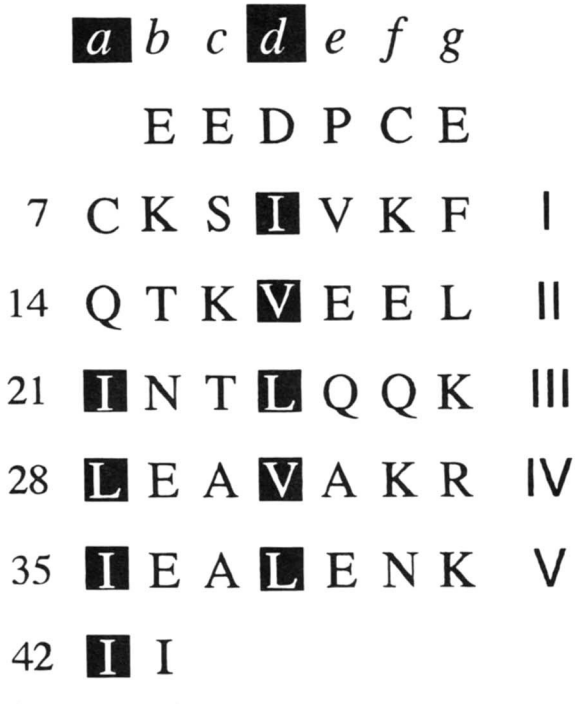

Fig. 1. The sequence of the C-terminal coiled coil domain (residues 451 to 492) of chicken CMP (Argraves et al., 1987). The five heptad repeats in the sequence of CMPcc (Hauser & Paulsson, 1994) are indicated by roman numerals to the right of the figure. Hydrophobic residues in the *a* and *d* positions of the heptads are highlighted. The protein used in the present studies contains the additional "foreign" N-terminal residues GSHM. These residues are an artifact of the expression system for CMPcc and are not included in the present numbering scheme.

Results

Determination of oligomerization state

For structural studies recombinant CMPcc was prepared by heterologous gene expression in *E. coli* (Materials and methods). The homogeneity of affinity purified recombinant CMPcc was assessed by tricine SDS-PAGE (Schägger & von Jagow, 1987). Analysis under reducing conditions (Fig. 2, lane 1) revealed a single band with a mobility consistent with the calculated molecular mass of the monomer (5,386 Da). Analysis under non-reducing conditions (Fig. 2, lane 1) revealed a band consistent with the calculated molecular mass for a trimer (16,158 Da).

Sedimentation coefficients of oxidized and reduced NEM-CMPcc were determined by sedimentation velocity at 56,000 rpm, and average molecular masses by sedimentation equilibrium centrifugation at 34,000 rpm, as described previously (Kammerer et al., 1995). Sedimentation velocity runs revealed sharp boundaries indicating homogeneity of the material, and this was supported by linear plots of the logarithm of absorbance versus r^2 (van Holde, 1985). Coefficients $s^0_{20,w}$ = 1.84 S and $s^0_{20,w}$ = 1.78 S were obtained for oxidized and reduced NEM-CMPcc, respectively, assuming a partial specific volume of 0.73 mL/g. Sedimentation equilibrium measurements at 34,000 rpm yielded average molecular masses of 16.7 kDa for oxidized CMPcc, and 18.2 kDa for reduced NEM-CMPcc. These values indicate a trimeric oligomerization state for both the reduced and oxidized forms of CMPcc.

NMR resonance assignments

NMR spectra (e.g., Fig 3A) contain only resonances corresponding to the primary sequence of the CMPcc monomers, pointing to an equivalent magnetic environment for each of the three polypeptide

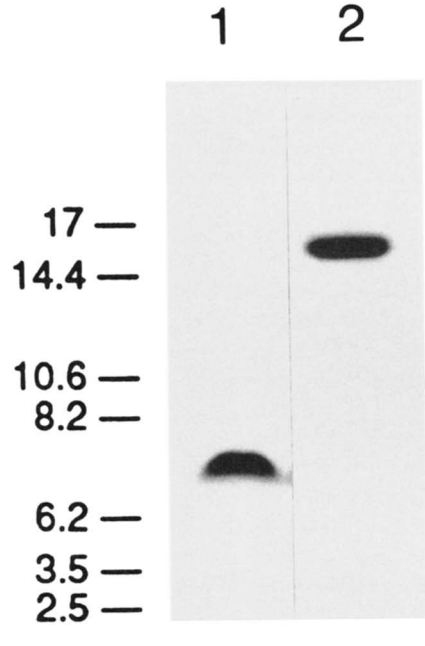

Fig. 2. Tricine-SDS-PAGE of purified recombinant CMPcc. Lanes: 1, reducing conditions; 2, non-reducing conditions. The migration of marker proteins of known molecular mass is shown to the left in units of kDa. Approximately 5 μg of protein were loaded in each lane.

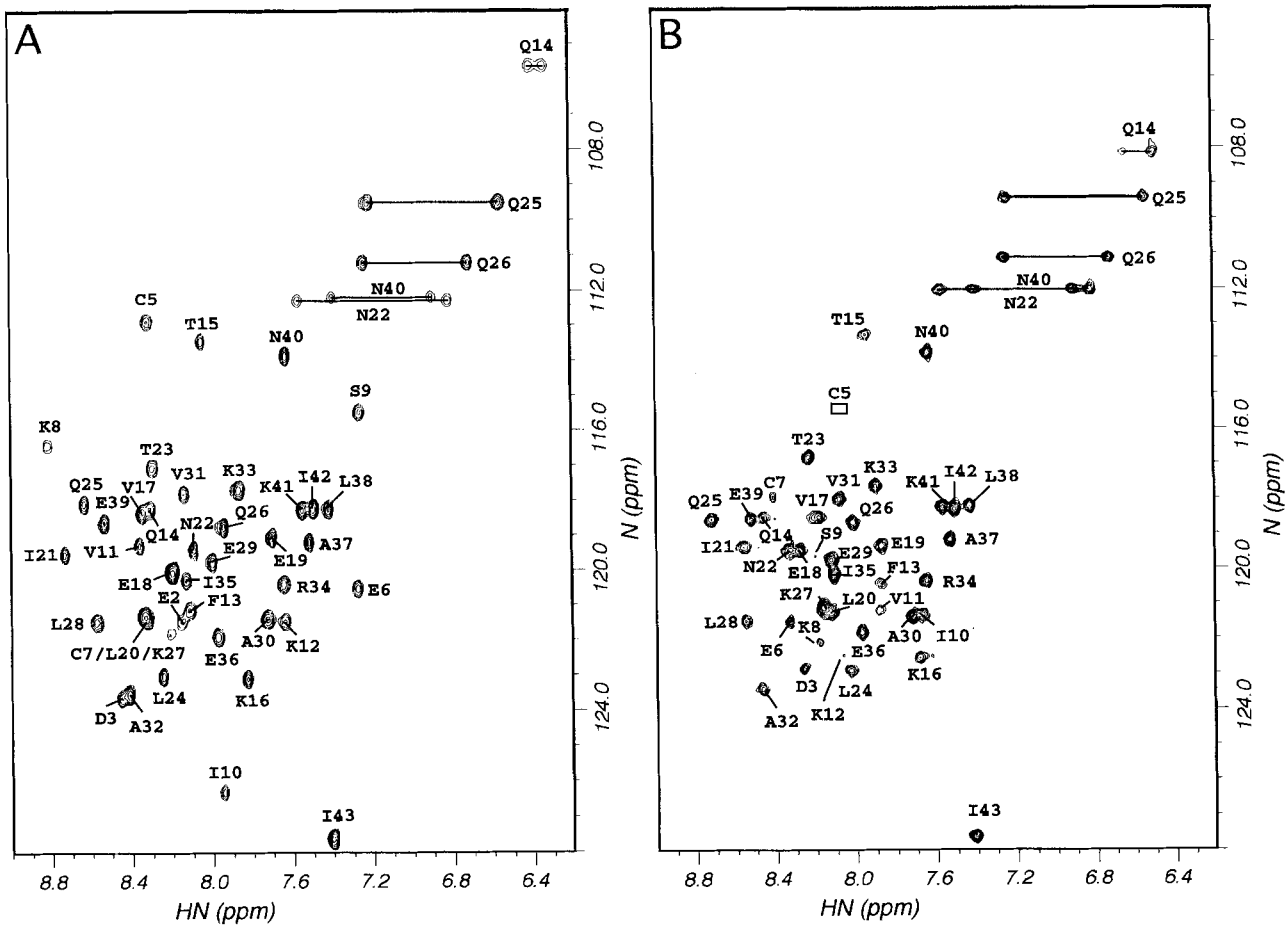

Fig. 3. ^{1}H-^{15}N HSQC spectra of (**A**) oxidized and (**B**) reduced CMPcc. The spectrum in (A) was obtained for a 3 mM solution of ^{15}N-labeled CMPcc in 90% H_2O/10% D_2O, 150 mM NaCl, pH 6.0. The spectrum in (**B**) was obtained for the same sample conditions, except with a 10-fold molar excess of DTT per CMPcc monomer. The box in (**B**) indicates the crosspeak for C5 which is only visible at lower contour levels.

chains. This observation indicates a parallel coiled-coil structure with threefold symmetry. A consequence of this threefold symmetry is that inter-chain disulfide bonds other than those between C5 and C7 are precluded; pairings such as C5–C5 or C7–C7 would result in two free cysteines per trimer, an arrangement inconsistent with the three-fold symmetry observed by NMR. Resonance assignments for CMPcc (Table 1) were obtained from a combination of 2D and 3D NMR spectra. CMPcc has an extremely high thermal stability, with a T_m above 100 °C in non-dissociating buffers (RAK and JE, unpubl. obs.). This high thermal stability made it possible to collect NMR data at a temperature of 50 °C, close to the upper temperature limit of our pulse field gradient probes. The use of high temperature circumvented many of the technical difficulties associated with NMR studies for a protein with a molecular weight of 16.2 kDa. For example, it was possible to obtain most "residue-type" assignments from a single 2D ^{1}H-TOCSY spectrum collected with a long isotropic mixing time of 60 ms. A distinct disadvantage for NMR work on CMPcc is the protein's very limited chemical shift dispersion; an observation that is likely to reflect the protein's predominantly α-helical structure, and the presence of only one aromatic residue (F13) in the sequence. Spectral overcrowding is particularly severe in the methyl region of the NMR spectrum, where hydrophobic V, I, L residues that form most of the interface between α-helices in the coiled coil resonate. Extensive assignments for most of the long-chain aliphatic spin-systems in CMPcc required the additional ^{13}C frequency handle provided by a 3D HCCH-TOCSY spectrum, to resolve the ambiguities inherent to the crowded ^{1}H-NMR spectrum.

Initial sequence-specific assignments were obtained from a long stretch of sequential HN-HN and HN-Hα NOE connectivities running from K8 to I43, identified in a ^{1}H 2D NOESY spectrum acquired with a high digital resolution. Subsequently, these assignments were confirmed in 3D ^{1}H-^{15}N NOESY-HSQC and HNCA spectra. An advantage of the 3D HNCA experiment is that it provides through-bond sequential connectivities, removing possible ambiguities in sequential assignments based on NOE distance information (Ikura et al., 1990). A second advantage of this experiment is that it provides Cα chemical shift information that can be used as a starting point for extending ^{1}H spin system assignments to ^{13}C resonances in 3D HCCH-TOCSY spectra.

Secondary structure

Chemical shift indices, and $^{3}J_{HNH\alpha}$ coupling constant values for CMPcc are summarized in Figure 4. Hα, Cα, and Cβ chemical shifts for residues K8 to N40 are consistent with an α-helical

Table 1. *^{15}N, ^{13}C, and ^{1}H resonance assignments for native CMPcc*

Residue	Chemical shift (ppm)						
	N	HN	Cα	Hα	Cβ	Hβ	Others
Gly −4			44.1	3.90			
Ser −3			58.6	4.56	64.4	3.85	
His −2			56.5	4.72	30.4	3.23,3.15	
Met −1		8.25	56.1	4.49	33.7	2.53,2.47	C_γ 32.1; H_γ 2.09,1.96; C_ϵ 17.6; H_ϵ 2.09
Glu 1		8.33	57.3	4.25	30.8	2.06,1.93	C_γ 36.6; H_γ 2.29
Glu 2	120.8	8.12	57.3	4.28	30.8	1.99, 1.88	C_γ 36.6; H_γ 2.29
Asp 3	123.5	8.41	52.0	4.91	42.0	2.88, 2.62	
Pro 4			64.4	3.85	32.9	2.30,1.87	C_γ 27.5; H_γ 1.95; C_δ 51.54; H_δ 3.93
Cys 5	112.9	8.30	54.4	4.36	41.6	3.67, 3.00	
Glu 6	120.5	7.27	56.5	4.30	30.8	2.23, 2.16	C_γ 37.5; H_γ 2.48
Cys 7	121.3	8.35	58.6	4.48	40.9	3.48, 2.96	
Lys 8	116.4	8.82	60.2	4.01	32.1	1.88, 1.96	C_γ 25.0; H_γ 1.52, 1.45; C_δ 29.6, H_δ 1.76,1.70; C_ϵ 42.4; H_ϵ 3.00
Ser 9	115.4	7.27	62.0	4.24	64.0	3.99, 4.18	
Ile 10	126.3	7.95	65.8	3.74	38.3	2.19	C_γ 30.4; H_γ 1.75; $C_{\gamma Me}$ 18.4; $H_{\gamma Me}$ 0.92; $C_{\delta Me}$ 17.25; $H_{\delta Me}$ 0.82
Val 11	119.3	8.36	67.1	3.54	31.7	2.01	$C_{\gamma Me}$ 21.3, 23.4; $H_{\gamma Me}$ 0.91, 0.98
Lys 12	121.4	7.66	60.2	4.05	32.5	2.02, 1.98	C_γ 25.0; H_γ 1.52; C_δ 25.9; H_δ 1.68; C_ϵ 42.9; H_ϵ 3.00
Phe 13	121.1	8.12	62.1	4.25	39.1	3.30, 3.28	H_δ 7.37; H_ϵ 7.42; H_ζ 7.24
Gln 14	118.2	8.31	59.6	3.54	27.9	1.48, 1.95	C_γ 33.7; H_γ 2.30; N_δ 105.6; H_δ 6.42, 6.33
Thr 15	113.4	8.05	66.5	3.96	69.8	4.24	C_γ 22.1; $H_{\gamma Me}$ 1.27
Lys 16	123.0	7.83	59.4	4.09	32.5	1.95	C_γ 25.0; H_γ 1.52, 1.28; C_δ 29.6; H_δ 1.74; C_ϵ 42.4; H_ϵ 2.90
Val 17	118.3	8.35	67.1	3.54	31.7	2.01	$C_{\gamma Me}$ 22.6, 24.2; $H_{\gamma Me}$ 0.90, 0.65
Glu 18	119.9	8.19	61.1	3.93	30.0	2.24, 2.14	C_γ 37.5; H_γ 2.64, 2.25
Glu 19	119.1	7.71	60.0	4.19	29.6	2.22	C_γ 36.6; H_γ 2.47, 2.25
Leu 20	121.3	8.33	59.0	4.13	42.9	1.44, 2.08	Cγ 27.1; Hγ 1.89; $C_{\delta Me}$ 23.8, 25.5; $H_{\delta Me}$ 0.93, 0.91
Ile 21	119.5	8.73	66.0	3.59	37.5	2.02	C_γ 30.0; H_γ 1.80, 1.00; $C_{\gamma Me}$ 18.0; $H_{\gamma Me}$ 0.94; $C_{\delta Me}$ 13.9; $H_{\delta Me}$ 0.78
Asn 22	119.4	8.09	57.3	4.54	38.7	3.02, 2.91	N_γ 112.2, H_γ 7.60,6.83
Thr 23	117.0	8.29	67.3	4.01	69.4	4.39	$C_{\gamma Me}$ 22.1; $H_{\gamma Me}$ 1.30
Leu 24	123.0	8.24	58.8	3.98	42.9	1.38, 2.08	C_γ 27.5; H_γ 1.97; $C_{\delta Me}$ 26.7, 24.2; $H_{\delta Me}$ 0.93, 0.87
Gln 25	118.1	8.64	60.4	3.92	28.1	2.38, 2.26	C_γ 35.0; H_γ 2.54, 2.41; N_δ 109.4; H_δ 7.24, 6.59
Gln 26	118.7	7.94	59.6	4.11	28.8	2.28, 2.23	C_γ 34.6; H_γ 2.46, 2.64; N_δ 111.7; H_δ 7.26, 6.74
Lys 27	121.3	8.33	60.0	4.13	33.3	2.02, 1.91	C_γ 25.9; H_γ 1.47; C_δ 26.3; H_δ 1.74, 1.67; C_ϵ 42.0; H_ϵ 2.90
Leu 28	121.5	8.57	58.4	4.04	42.0	1.90, 1.71	C_γ 28.3; H_γ 1.74; $C_{\delta Me}$ 25.0, 26.3; $H_{\delta Me}$ 0.93, 0.93
Glu 29	119.7	8.01	59.6	4.09	29.6	2.17	C_γ 37.0; H_γ 2.35, 2.44
Ala 30	121.4	7.72	55.7	4.19	18.4	1.60	
Val 31	117.8	8.13	66.9	3.73	31.7	2.30	$C_{\gamma Me}$ 22.1, 23.0; $H_{\gamma Me}$ 0.95, 1.11
Ala 32	123.5	8.42	56.1	3.96	18.0	1.52	
Lys 33	117.7	7.86	59.2	4.12	32.5	1.99, 1.93	C_γ 25.5; H_γ 1.55; C_δ 28.8; H_δ 1.71, 1.58; C_ϵ 42.4; H_ϵ 3.00
Arg 34	120.4	7.64	59.4	4.16	32.1	2.12, 2.01	C_γ 27.1; H_γ 1.80; C_δ 44.9; H_δ 3.36, 2.96
Ile 35	120.3	8.12	64.8	3.74	38.3	1.93	C_γ 30.4; H_γ 1.78, 0.89; $C_{\gamma Me}$ 18.0; $H_{\gamma Me}$ 0.89; $C_{\delta Me}$ 16.0; $H_{\delta Me}$ 0.84
Glu 36	121.9	7.97	59.6	4.10	30.4	2.18	C_γ 36.6; H_γ 2.22, 2.40
Ala 37	119.2	7.51	55.3	4.17	18.4	1.51	
Leu 38	118.2	7.42	58.2	4.07	42.9	1.45, 2.06	C_γ 27.1, H_γ 1.95; $C_{\delta Me}$ 26.7, 24.2; $H_{\delta Me}$ 0.93, 0.87
Glu 39	118.6	8.53	59.4	3.85	30.0	1.95, 2.34	C_γ 37.9; H_γ 2.53, 2.25
Asn 40	113.8	7.63	54.8	4.62	39.5	2.88, 2.84	N_γ 112.1; H_γ 7.41, 6.91
Lys 41	118.2	7.54	57.5	4.36	34.1	1.94	C_γ 25.4; H_γ 1.53; C_δ 29.6; H_δ 1.68; C_ϵ 42.8; H_ζ 3.00
Ile 42	118.2	7.49	61.5	4.26	38.7	1.95	C_γ 27.5; H_γ 1.53, 1.28; $C_{\gamma Me}$ 18.0; $H_{\gamma Me}$ 0.91; $C_{\delta Me}$ 13.9; $H_{\delta Me}$ 0.85
Ile 43	127.6	7.40	63.3	4.05	39.9	1.86	C_γ 27.9; H_γ 1.45, 1.18; $C_{\gamma Me}$ 18.4; $H_{\gamma Me}$ 0.92; $C_{\delta Me}$ 13.5; $H_{\delta Me}$ 0.87

[a]Chemical shifts for stereospecifically assigned resonances are underlined. The atom with the lower branch number (PDB convention) is shown first (e.g. $H_\beta 1$, $H\gamma_{Me}1$). Stereospecific assignments for Hβ protons were obtained on the basis of 50-ms mixing time NOE, and 3D HNHB data (Archer et al., 1991). Stereospecific assignments for Val and Leu methyl groups were obtained by the method of Neri et al. (1989).

structure, and show large deviations from the "coil" values of Wishart et al. (1995a). Indeed, most residues between K8 and N40 (75%) have Cα chemical shift values well downfield of the 90% confidence intervals for α-helices in globular proteins (Wishart et al., 1991). The strong α-helix shifts of Cα resonances in CMPcc could reflect a distinct feature of coiled coils, or could be a statistical artifact of the relatively small database of $^{13}C\alpha$ chemical shifts (Wishart et al., 1991). Hα chemical shifts are within 90% limits for α-helices, while for Cβ shifts only mean values are available (Wishart et al., 1995a). All resolvable $^{3}J_{HNH\alpha}$ coupling constants between residues K8 and N40 are below 5.5 Hz, as expected for an α-helical structure.

Symmetric oligomers present a severe challenge for NMR studies because of the difficulties associated with distinguishing NOE

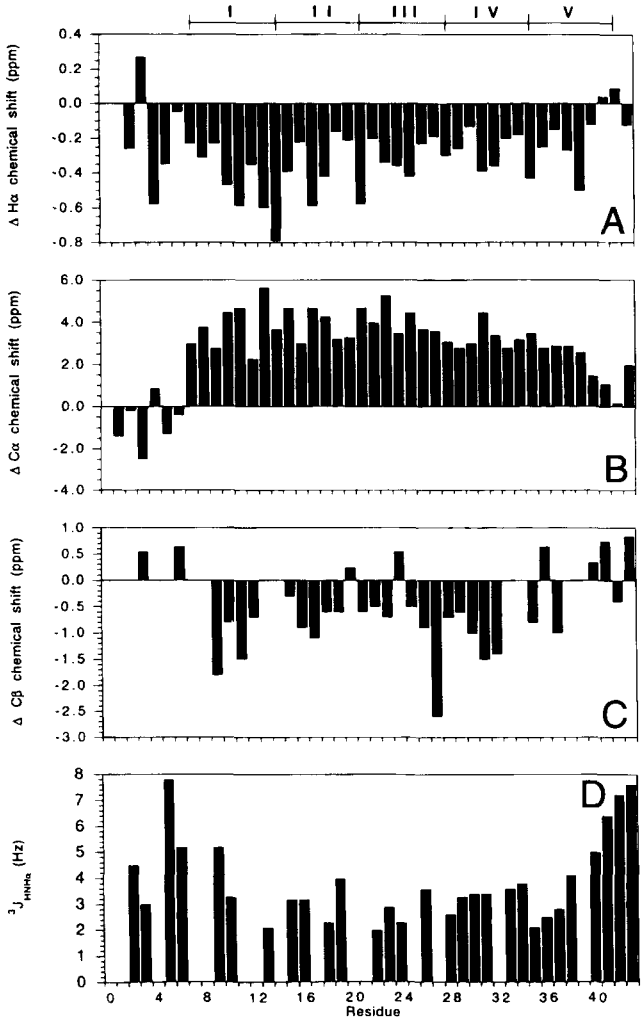

Fig. 4. Differences in Hα (**A**), Cα (**B**), and Cβ (**C**) chemical shifts from random coil values (Wishart et al., 1995a), and $^3J_{HNH\alpha}$ coupling constants (**D**) for native (oxidized) CMPcc. The five heptad repeats in the sequence of CMPcc are indicated by roman numerals at the top of the figure. $^3J_{HNH\alpha}$ coupling constants were measured from a 3D HNHA spectrum by the method of Vuister and Bax (1993).

distance contacts within a chain from those between chains (Folkers, et al., 1993; O'Donoghue et al., 1993; Junius et al., 1996). One strategy to differentiate inter-chain from intra-chain NOEs is to make oligomers that consist of 1:1 mixtures of isotopically labeled and unlabeled monomers. Inter-chain NOEs can then be distinguished from intra-chain NOEs by using NMR spectral editing techniques that select for magnetization transferred from protons on labeled chains, to protons on unlabeled chains (Folkers, et al., 1993). Using this strategy in conjunction with isotope-filtered NOESY experiments (Kay et al., 1990; Lee et al., 1994) we were able to detect inter-chain NOEs for ^{13}C bound protons, which are mostly consistent with the predicted packing of *a* and *d* residues in the interface of a parallel coiled coil (R. Wiltscheck, S.A. Dames, & A.T. Alexandrescu, unpubl. obs.). In the case of ^{15}N bound protons, however, we did not observe any inter-chain NOEs. The X-ray structure of the parallel three-stranded coiled coil GCN4-PII (Harbury et al., 1994) serves as a useful benchmark for the structure of a trimeric coiled coil. The NOE is primarily sensitive to distances shorter than 5 Å. Using the X-ray structure of GCN4-PII as a model for a trimeric coiled coil we searched for all distances less than 5 Å that involve protons on different chains. Per monomer, there are on average about 650 inter-chain distances shorter than 5 Å between carbon bound protons. For distances involving amide protons, however, this number drops to about 10 per monomer. Furthermore, most of the inter-chain distances involving amide protons are not consistently below 5 Å when different chains of the GCN4-PII trimer are examined. Lattice packing often induces small deviations from perfect symmetry in X-ray structures of oligomeric proteins. That the few inter-chain distances less than 5 Å involving amide proton are not conserved when different chains of the GCN4-PII trimer are compared, suggests that these contacts occur predominantly in regions of the X-ray structure where deviations from threefold symmetry are pronounced. Taken together, these observations suggest that in a trimeric coiled coil backbone amide protons are insulated from the trimer interface by the hydrogen bonding network of the α-helix monomers. Inter-chain NOEs involving backbone amide protons are thus expected to be extremely rare in a trimeric coiled coil, consistent with our isotope-filter NOESY data.

Intra-chain HN-HN and HN-Hα NOE connectivities observed in 2D NOESY and 3D ^1H-^{15}N NOESY-HSQC spectra of CMPcc are summarized in Figure 5A. Residues K8 to I43 give, for the most part, strong to medium *dNN*, and medium to weak *dαN* NOE connectivities. A long stretch of $dNN(i,i+2)$, $d\alpha N(i,i+2)$, $d\alpha N(i,i+3)$, and $d\alpha N(i,i+4)$ connectivities indicate a continuous α-helix for this region of the polypeptide chain. The three C-terminal residues K41 to I43 show some NOEs characteristic of α-helical structure. Chemical shifts and $^3J_{HNH\alpha}$ coupling constants, however, suggest that these residues undergo rapid averaging between α-helical and unstructured conformations. Taken together the NOE, chemical shift, and $^3J_{HNH\alpha}$ coupling constant data suggest that residues K8 to N40 define the approximate limits of α-helix secondary structure of the CMPcc monomers. Severe spectral overlap precluded a detailed analysis of structure between C5 and C7. With the possible exception of a reverse turn involving residues E2-D3-P4-C5, we did not detect any regular secondary structure upstream of residue C7.

Comparison of oxidized and reduced CMPcc

Figure 3B shows a ^1H-^{15}N HSQC spectrum of CMPcc in the presence of a 10-fold molar excess (per monomer) of the reducing agent dithiothreitol (DTT). Because the resonances of the oxidized and reduced forms of CMPcc are in slow exchange on the chemical shift time scale, the spectrum of the reduced protein was assigned independently using 3D TOCSY-HSQC and 3D NOESY-HSQC data. HN and Hα chemical shift differences between the two forms of the protein are summarized in Figure 6. A chemical shift difference gradient that decays by one-half for about every nine residues runs from the N- to the C-terminus of the molecule. Consequently, chemical shifts downstream of L25 are highly similar between the oxidized and reduced protein (Figs. 3 and 6). Indeed, these served as a useful starting point for sequential assignment of the reduced protein. Larger chemical shift differences are observed near the N-terminus, together with a decrease in intensity of ^1H-^{15}N crosspeaks in the reduced protein. An unfolding of α-helical structure upon reduction of the disulfide bonds should give a uniform trend of chemical shifts towards random coil values. Instead, a periodicity in chemical shift differences of about

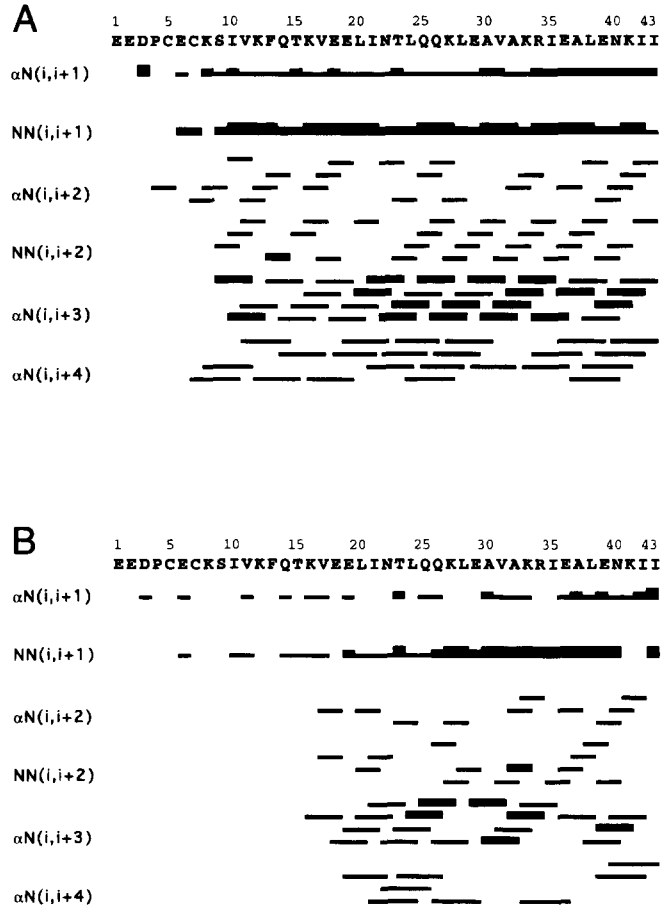

Fig. 5. Summary of short-range *dNN* and *dαN* connectivities in native (**A**) and reduced (**B**) CMPcc. The thickness of the bars indicates the intensity (strong, medium, weak) of the observed NOEs.

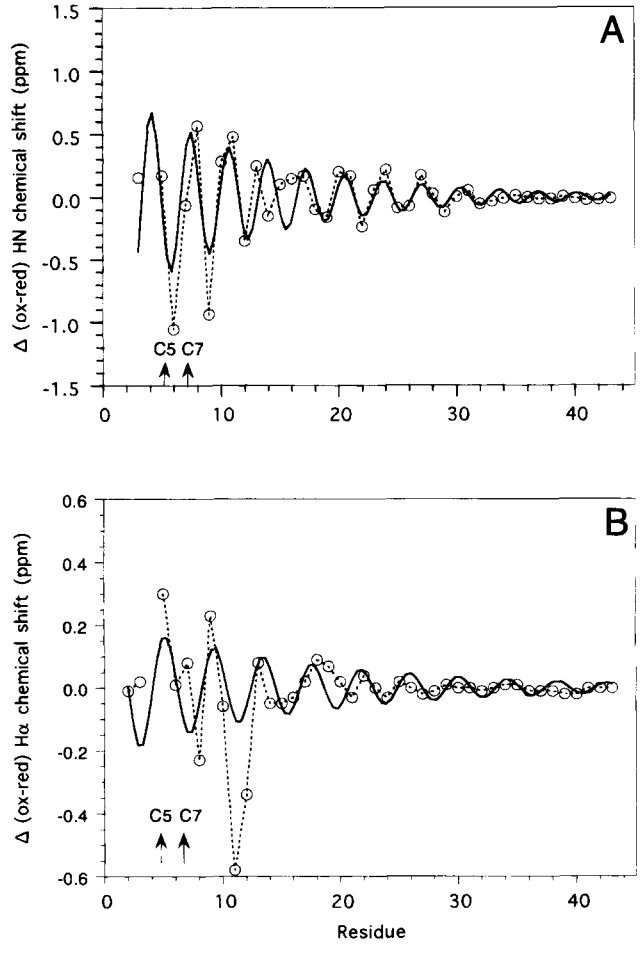

Fig. 6. Differences in HN (**A**), and Hα (**B**) chemical shifts between native and reduced CMPcc. Dotted lines connect the residues in the sequence and are intended only to guide the eye. Solid lines represent nonlinear least-squares fits of the data to the damped cosine function

$$y = K_0\left[\cos\left(\frac{2\pi(x)}{\lambda}\right) - \Delta\right]\exp^{-(x/m)}$$

with the free variables: K_0—a constant describing the chemical shift difference for the first residue, Δ—an arbitrary phase shift, λ—the period of the sinusoidal function, and m—a constant that describes the decay of the sinusoidal function as a function of position in the sequence. Values for (**A**) were λ = 3.3 residues, m = 12.0 residues, with an R correlation coefficient of 0.66; for (**B**) λ = 4.2 residues, m = 16.2 residues, and R = 0.48. Reduced χ^2 values for both fits were within 95% confidence limits (Shoemaker et al., 1981).

three to four residues is observed. This periodicity may reflect the 3.5 residue per turn periodicity of an α-helix in a coiled coil (Cohen & Parry, 1990) and could be due to changes in the solvent environment of the asymmetric knobs-into-holes interface between any two adjacent monomers (Harbury et al., 1994). Alternatively the periodicity could simply reflect changes in the inside/outside polarity of C5 and C7 relative to the amphipatic helix monomers upon reduction of the protein.

Residues I10 to V17 show strong protection in $^1H/^2H$ isotope exchange experiment with the oxidized protein (Fig. 7A) but no protection in the reduced protein (Fig. 7B). A dramatic difference is also evident when NOE data for residues I10 through V17 are compared in the oxidized and reduced forms of the protein. In the reduced protein, residues I10 to V17 show a decrease in NOE's characteristic of α-helical structure (Figs. 5 and 8D) at the expense of intense NOEs to the water resonance at 4.49 ppm. In the absence of DTT, similar NOEs to water are observed only for residues E2, D3, E6 upstream of the disulfide bonds, and for residue S9. In principle, NOEs to water could arise from dipolar contacts between amide protons and protein-bound water. For reduced CMPcc, however, this mechanism is extremely unlikely. First, it is difficult to envisage a structure where protein-bound waters are segregated to a discrete portion of the polypeptide chain (e.g., residues D3 to V17). Second, the magnitude of the NOEs would require prohibitively short distances between amide protons and water, as the water NOE crosspeaks are comparable or stronger than the auto-correlation peaks. The most likely explanation for the observed NOEs is chemical exchange mediated magnetization transfer between amide protons and water. For this type of NOE effect to be observed, the rate of chemical exchange must be comparable to that of proton R_1 relaxation. This puts a limit of approximately 0.1 s^{-1} to 10 s^{-1} on the rates of amide exchange (Forsén & Hoffman, 1963), and limits between 0.1 and 200 on the protection factors of residues I10 to V17 in the reduced protein. Marginal protection from solvent exchange, however, does not necessarily imply a lack of structure (Alexandrescu et al., 1996).

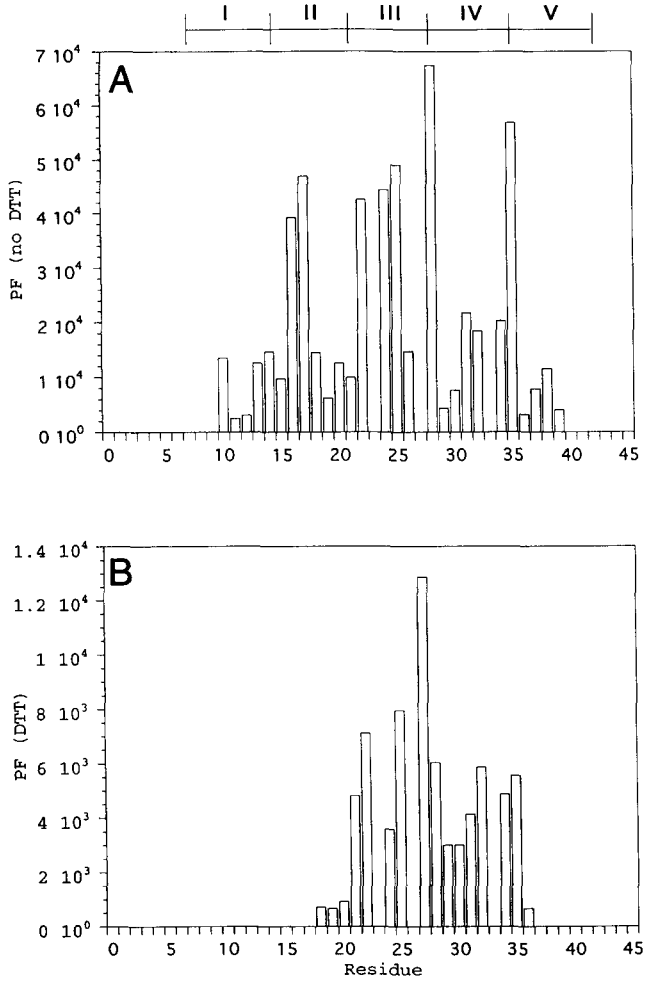

Fig. 7. Hydrogen exchange protection factors for (**A**) oxidized and (**B**) reduced CMPcc. The subset of slowest exchanging residues have similar protection factors in spite of disparate intrinsic exchange rates, suggesting an *EX2* exchange mechanism (Bai et al., 1995).

Chemical exchange between amide protons and water provides an extremely efficient relaxation sink for residues D3 to V17, with the quality of the NOE spectrum showing an increasing deterioration from V17 toward the N-terminus of the reduced protein (Fig. 8D). Consequently, a detailed NMR structural analysis of residues I10 to V17 in the reduced protein is precluded under the conditions of this study. A 3D NOESY-HSQC spectrum collected for the reduced protein at a lower temperature of 27 °C shows some improvment in the data for residues V17 to F13 as a result of attenuated solvent exchange effects at the lower temperature. There is an increase in the intensity of $d\alpha N(i, i + 3)$ NOEs in the region between N22 and T15 at the lower temperature, and we detected the additional NOEs dNN(T15,V17), $d\alpha N$(F13,T15), $d\alpha N$(T15, E19), and $d\alpha N$(K12,K16). These NMR data suggest that α-helical structure in the reduced protein may extend to about residue F13 at a temperature of 27 °C. Even in the spectrum collected at 27 °C, however, NOEs to water become increasingly large upstream of F13. These solvent exchange effects preclude an NMR comparison of α-helical structure upstream of F13 in the reduced and oxidized proteins. There are a number of observations, however, which suggest that even at 50 °C α-helical structure may be significantly populated for residues I10 to V17 in the reduced protein. Hα chemical shifts remain within the range predicted for α-helical structure (Wishart et al., 1995a). The reduced protein exhibits a 5% smaller negative ellipticity at 222 nm, and less than a 1% reduction in negative ellipticity at 208 nm compared to the oxidized protein (Fig. 9). A complete loss of α-helical structure for residues I10 to V17 would correspond to a 26% loss of the total α-helix structure identified by NMR for oxidized CMPcc. The magnitude of the changes observed in the CD spectrum seem to preclude a complete unfolding of residues I10 to V17 in the reduced protein.

In a separate study, Beck et al. (1996) studied a trimeric peptide that contained all of the sequence of the homologous human CMPcc domain downstream of the disulfide bonds. CD spectra of this peptide suggested that it was almost fully helical (Beck et al., 1996), consistent with the CD data on the reduced chicken CMPcc in this study. Finally, we have synthesized a peptide containing residues K16 to K41 of chicken CMPcc (with blocked C-and N-termini). Analytical ultracentrifugation studies of this peptide, which includes the entire subset of residues that are protected from solvent exchange in the reduced protein, indicate that it forms a mixture of trimers and higher order oligomers. The second heptad repeat of CMPcc contains a Gln residue in its *a* position. Coiled-coil trimers show enrichment for Gln residues in the first position of heptad repeats when compared to dimers (Woolfson & Alber, 1995), and it has been suggested that Gln residues in *a* positions may specify trimeric over dimeric oligomerization states (Gonzalez et al., 1996). In spite of the high flexibility observed for residues V17 to I10 in reduced CMPcc, Q14 or other residues in this sequence appear to play a role in the specificity of trimer formation.

Discussion

The C-terminal domain of CMP forms a trimeric coiled coil in which the α-helical chains are covalently linked by disulfide bonds between residues C5 and C7. NMR data indicate magnetically equivalent environments for each of the CMPcc monomers. This indicates a parallel structure, with a threefold symmetry axis perpendicular to the long axis of the coiled coil. NOE, chemical shift, $^3J_{HNH\alpha}$ coupling constant, and hydrogen exchange data suggest that α-helix secondary structure of the monomers extends from about residue K8 to N40. The threefold symmetry of the trimer is maintained when the inter-chain disulfide bonds are reduced by a 10-fold molar excess of DTT. Comparison of hydrogen exchange rates in reduced and oxidized CMPcc suggest that the inter-chain disulfide bonds have a role in restricting the flexibility of the coiled coil.

Coiled-coil domains in extracellular proteins are frequently flanked by pairs of closely spaced cysteines that form inter-chain disulfide bonds (Kammerer, 1997). The observation that these occur at the N- or C-terminal ends of coiled coil domains may reflect that inter-chain disulfide bonds cannot be easily accommodated in a regular coiled coil structure. To examine whether inter-chain disulfide bonds with the C_f-X_g-C_a spacing found in CMPcc are compatible with a trimeric coiled-coil structure, we modeled two cysteine residues in the *f* (S14) and *a* (I16) positions of the X-ray structure of GCN4-PII (Harbury et al., 1994). Assuming a regular coiled coil structure ($\phi \approx -60°$, $\psi \approx -40°$), the $\chi 1$ dihedral angles of the two cysteines are the only free variables that affect the distance between the Sγ atoms from neighboring chains. Typical distances for Sγ atoms in disulfide bonds are of the order of 2.0 Å. The minimum Sγ-Sγ distance as a function of the two $\chi 1$

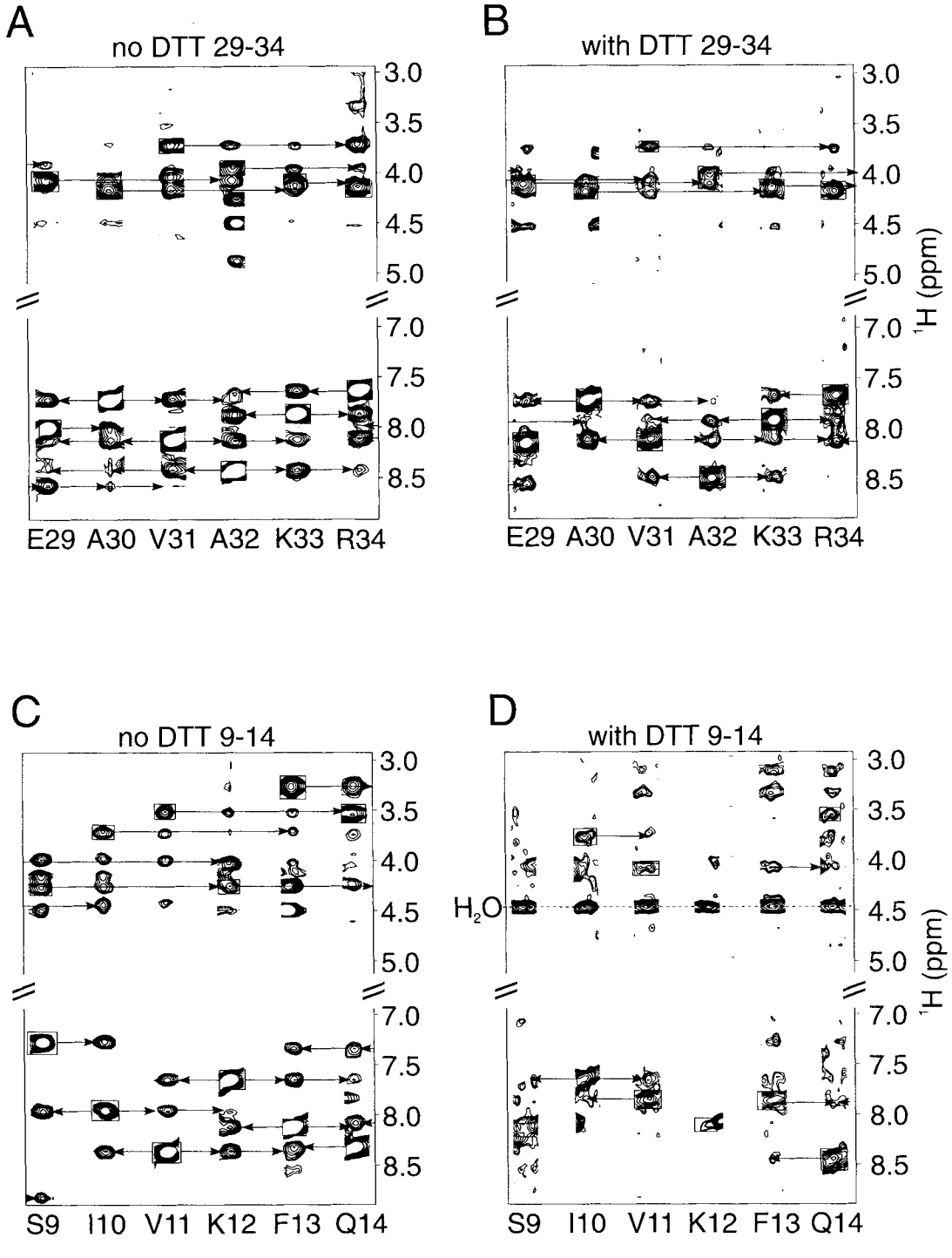

Fig. 8. Strips taken from ^{1}HN-^{1}H planes (ω3-ω1) of 3D ^{1}H-^{15}N NOESY HSQC spectra. The spectra compare NOE connectivities for residues E29 to R34 and S9 to Q14 in oxidized (**A, C**) and reduced (**B, D**) CMPcc. Arrows indicate HN-HN and HN-Hα NOE connectivities characteristic of α-helical structure. The label "H_2O" in (D) indicates a series of residues in the reduced protein that show very strong NOEs to the water resonance at 4.49 ppm. We attribute these NOEs to magnetization transfer mediated by hydrogen-exchange on a time scale between 0.1 and 10 s. In (**C**), the NOE to water in the strip for F13 is due to the overlapping signal of E2, while the weak NOE to water for S9 is genuine. The spectral region between 5 and 7 ppm indicated by breaks along the *y*-axis contains no signals.

dihedral angles in this modeling experiment, however, was closer to 9.0 Å. This suggests that the interchain disulfide bonds of CMPcc are incompatible with a trimeric coiled coil structure, an observation consistent with the NMR data that indicates that α-helical structure in CMPcc does not extend upstream of residue K8. In this regard, it is interesting to note that residues P4 and D3 immediately upstream of the disulfide bonds between C5 and C7, afford a very strong α-helix N-cap signal (Richardson & Richardson, 1988).

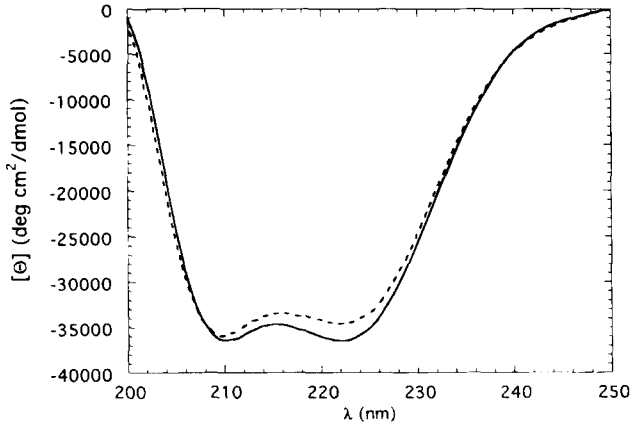

Fig. 9. Far-UV CD spectra of oxidized CMPcc (thick line) and reduced NEM-CMPcc (dashed line). The spectra were recorded at a temperature of 50 °C and contained 6.8 μM CMPcc and 5.4 μM NEM-CMPcc trimer, respectively, in 5 mM Na_2HPO_4 buffer supplemented with 150 mM NaCl, pH 7.4.

The inter-chain disulfide crosslinks stabilize the coiled-coil structure of CMPcc. Estimates of the stability to unfolding can be obtained from the hydrogen exchange data for reduced and oxidized CMPcc. Under *EX2* conditions, the rate of hydrogen exchange k_{ex} is given by the product of the equilibrium constant K_{op} = [open]/[closed] and the intrinsic exchange rate k_{int}:

$$k_{ex} = k_{int} K_{op}$$

where "open" and "closed" refer to exchange susceptible and exchange resistant (e.g., hydrogen bonded) conformations, respectively. The intrinsic rate k_{int} for hydrogen exchange in an unstructured conformation depends on a number of factors such as temperature, pH, and sequence effects; and can be estimated from model peptides (Bai et al., 1993). The protection factor (P_f) values in Figure 7 represent hydrogen exchange rates normalized for intrinsic rates, and are related to K_{op} by

$$\frac{1}{P_f} = K_{op} = \frac{k_{ex}}{k_{int}}.$$

The largest protection factors observed in Figure 7 should reflect hydrogen exchange by a global unfolding mechanism, with $K_{op} = K_{unfolding}$ (Bai et al., 1995). For the oxidized protein the highest P_f values are in the range between 40,000 and 70,000. From $\Delta G_u = -RT \ln K_{op}$ it is possible to calculate a value for 7.0 ± 0.1 kcal/mol for the free energy of unfolding of the oxidized protein at a temperature of 50 °C. For the reduced protein the highest P_f values are in the range between 6,000 and 13,000 corresponding to a ΔG_u of 5.8 ± 0.3 kcal/mol. We can thus estimate that the inter-chain disulfide bonds between C5 and C7 stabilize CMPcc by about 1 kcal/mol under the conditions of the present study: 2.6 mM protein, pH 6, and 50 °C. Both the oxidized and reduced protein are extremely stable. The stability of the reduced protein, however, is expected to be concentration dependent (Kammerer et al., 1995). A possible advantage conferred by the disulfide crosslinks is to abolish this concentration dependence of stability (Antonsson et al., 1995).

NMR data indicate that the α-helical coiled-coil structure is conserved for at least residues I21 to N40 in the reduced protein. An NMR analysis of residues upstream of E18 in the reduced protein is made difficult by extremely rapid hydrogen exchange that quenches the intensity of amide proton resonances from this region of the protein. CD and chemical shift data, however, suggest similar contents of α-helical structure for the oxidized and reduced proteins. The lack of protection from solvent exchange observed for residues I10 through V17 in the reduced protein is more likely to reflect an increase in flexibility that transiently leaves amide protons in this region of the protein more accessible to solvent, rather than an unfolding of α-helical structure upon reduction of the inter-chain disulfide bonds. Residues C7 to F13 of CMPcc (Fig. 1) show strong deviations from the consensus sequence of a heptad repeat. Position *a* is occupied by a cysteine, while positions *e* and *g* are occupied by hydrophobic valine and phenylalanine residues, respectively. The frequencies of these residues in their respective positions is extremely small in the database of known coiled coil sequences (Lupas et al., 1991; Woolfson & Alber, 1995). The high flexibility of the region upstream of E18 may be inherent to the unusual sequence of the first heptad repeat. The inter-chain disulfide bonds may prevent transmission of this flexibility to the domains upstream of the coiled coil in the intact CMP protein, and/or protect the coiled coil domain from proteolytic degradation.

Materials and methods

Sample preparation

The gene for CMPcc was generated from an *AmpliTaq* DNA polymerase (Roche Molecular, Bradford NY) extension of two synthetic 75-mer oligonucleotides, that contained a complementary 3′-overhang of 21 nucleotides: 5′-GAAGAAGATCCGTGCGAA TGCAAAAGCATCGTGAAATTCCAGACCAAAGTGGAAGAA CTGATCAACACCCTGCAG-3′ and 5′-GATGATTTTGTTTTCC AGCGCTTCGATACGTTTCGCCACCGCTTCCAGTTTCTGCT GCAGGGTGTTGATCAGTTC-3′. Oligonucleotide sequences were based on the codon usage for highly expressed genes in enteric bacteria (Gribskov et al., 1984). Additional PCR primers 5′-CCTCCCATATGGAAGAAGATCCGTGCGAATG-3′ and 5′-CCC GGATCCTAGATGATTTTGTTTTCCAGCGC-3′ were used to insert a *Nde I* site at the 5′ end, and a *BamH I* site and TAG stop codon at the 3′ end, respectively. The amplified product was ligated into the *Nde I-BamH I* sites of the pET-15b expression vector (Novagen, Madison, WI). Recombinant insert DNA was verified by Sanger dideoxy sequencing. The sequence of the resulting CMPcc protein used in this study contains the four "foreign" residues GSHM at its N-terminus due to the thrombin cleavage site, and the *Nde I* restriction site. These residues are designated G(−4) to M(−1) in our numbering scheme, to emphasize that only residue E1 to I43 correspond to the true CMPcc domain. While amide proton resonances were not observed for these first four "foreign" residues (Fig. 3A), 3D HCCH-TOCSY data enabled some of the aliphatic proton and carbon spin-systems to be assigned in the case of the oxidized protein (Table 1).

E. coli BL21(DE3) host strain (Novagen), which has the gene for bacteriophage T7 RNA polymerase integrated into its chromosome (Studier et al., 1990), was used for all expression experiments. Isotopic labeling with ^{15}N and ^{13}C was carried out at 37 °C in modified New Minimal Medium (Budisa et al., 1995): 55 mM

KH_2PO_4, 100 mM K_2HPO_4, 10 mM Na_2SO_4, 20 mM NH_4Cl (^{14}N or ^{15}N); 16 mM glucose (^{12}C or ^{13}C), 1 mM $MgSO_4$, 1 mg/L Ca^{2+}, 1 mg/L Fe^{2+}, 1 μg/L Cu^{2+}, 1 μg/L Mn^{2+}, 1 μg/L Zn^{2+}, 1 μg/L MnO_4^{2-}, 10 mg/L thiamine, 10 mg/L biotin, supplemented with 100 μg/mL ampicillin. For the production of unlabeled CMPcc, bacteria were grown at 37 °C in LB medium containing 100 μg/mL ampicillin. Cells were induced with 1 mM IPTG after growth to an OD_{600} of 0.8, and incubated for a further 12 h.

Purification of 6xHis-tagged protein by affinity chromatography on Ni^{2+}-S-sepharose (Novagen) was performed under denaturing conditions as described in the manufacturer's instructions. The 6xHis-tag was removed by proteolytic cleavage for 4 h at room temperature using a concentration of five units of human thrombin per 1 mg of His-tagged protein, in thrombin cleavage buffer (20 mM Tris-HCl pH 8.4, 150 mM NaCl, 2.5 mM $CaCl_2$). The identity of the protein was confirmed by nine cycles of N-terminal protein sequencing and amino acid composition analysis. Reduced NEM-CMPcc was prepared according to previously published methods (Kammerer et al., 1995).

NMR spectroscopy

NMR spectra were acquired on a Varian *UNITY+* 600 MHz spectrometer, with the probe thermostated at 50 °C. The experiments employed were 2D NOESY; 2D TOCSY ; 2D ^1H-^{15}N HSQC; 3D ^1H-^{15}N-NOESY-HSQC; 3D ^1H-^{15}N TOCSY-HSQC; 3D HNCA; 3D HCCH-TOCSY; 3D HNHA; 3D HNHB. A 4 mM CMPcc sample (pH = 5.5) was used for homonuclear 2D spectra (NOESY, TOCSY). ^{15}N-separated experiments (HSQC, NOESY-HSQC, TOCSY-HSQC, HNHA, HNHB) were recorded on a 3 mM sample of uniformly ^{15}N-labeled CMPcc (pH = 6.0). A 1 mM sample of uniformly $^{15}N/^{13}C$-double labeled CMPcc (pH = 5.7) was used for 3D HNCA and HCCH-TOCSY experiments. Unless indicated, all samples were dissolved in 90% H_2O/10% D_2O, containing 150 mM NaCl.

Mixing times of 100 ms were used for all NOE experiments. 2D TOCSY, 3D ^1H-^{15}N TOCSY-HSQC, and 3D HCCH-TOCSY experiments employed isotropic mixing times of 60, 40, and 24 ms, respectively, achieved by use of a DIPSI-2 sequence (Shaka et al., 1988). In the 3D HNCA experiment the ^{13}C transmitter power was optimized for a B_1 field of 5.2 kHz to selectively excite the α-carbon resonances. In the HCCH-TOCSY experiment, a B_1 field of 8.9 kHz was necessary to obtain a uniform excitation of all aliphatic carbon resonances. Carbonyl decoupling in HNCA and HCCH-TOCSY was achieved by a 180° pulse with a SEDUCE shape profile (McCoy & Mueller, 1992), and an RF field strength of 2.0 kHz. GARP ^{15}N decoupling (Shaka et al., 1985) during acquisition was applied for all heteronuclear experiments, except HCCH-TOCSY where a WALTZ-16 pulse sequence (Shaka et al., 1983) was used for ^{13}C decoupling. Frequency discrimination in indirect dimensions was achieved using TPPI-STATES phase cycling (Marion et al., 1989). A low-power presaturation pulse during the recycling delay of 1.2 s was used for solvent suppression in the 2D NOESY and TOCSY experiments, and in the 3D HNHA experiment. All other experiments employed pulse field gradients (Kay, 1995) for solvent suppression (Bax & Pochapsky, 1992), and coherence selection (Davis et al., 1992). Pulse field gradient spectra were processed by the method of Kay et al. (1992). An internal DSS standard was used for spectral referencing of proton signals. ^{15}N and ^{13}C reference frequencies were calculated from the ^1H frequency of DSS in water, as described by Wishart et al. (1995b).

A series of ^1H-^{15}N gradient enhanced HSQC spectra were collected to follow the titration of a 1 mM ^{15}N-labeled sample of CMPcc with 0, 1, 2, 4, 8, 16, and 32 mM DTT. Resonances from the native protein decreased and resonances from the reduced protein increased, with increasing concentration of DTT. This observation indicates slow exchange between the two forms of the protein on the chemical shift time scale. The approximate midpoint of the transition occurred at a 4:3 molar ratio of DTT per CMPcc monomer. At a molar ratio of 16:3, native protein resonances were no longer detectable; higher concentrations of DTT produced no further changes in the protein's NMR spectrum. NMR assignments of reduced CMPcc were obtained for a 1 mM ^{15}N-labeled sample of CMPcc trimer containing a 10-fold molar excess of DTT (32 mM) per monomer of CMPcc, at a pH value of 5.8. 3D ^{15}N-separated TOCSY-HSQC and NOESY-HSQC spectra were collected as described for the native protein, with modifications to circumvent the decreased dispersion in the reduced protein. A reduced ^{15}N spectral width of 1000 Hz was used in order to optimize resolution by folding of well-dispersed amide protons. The number of increments in the ^{15}N dimension was reduced to 13 for the 3D NOESY-HSQC, and to 16 for the 3D TOCSY-HSQC experiment.

Hydrogen exchange

Hydrogen exchange rates were obtained at a temperature of 50 °C for two separate 2.6 mM samples of ^{15}N-labeled CMPcc: one without DTT, the second with a eightfold molar excess of DTT (64 mM) per CMPcc monomer. The pH values of the samples measured after completion of the experiments were 6.2 for the sample without DTT, and 5.8 for the sample containing DTT. Hydrogen exchange was initiated at a temperature of 20 °C by dissolving freshly lyophilized samples of CMPcc in 0.3 mL of 99.99% D_2O, or in a D_2O solution containing DTT. The samples were taken up in a micro-cell NMR tube (Shigemi), and inserted into the NMR probe that was pre-equilibrated to a temperature of 50 °C. The five-minute period between dissolution of the protein in D_2O and transfer to the NMR probe was not considered in calculating exchange rates, with the assumption that exchange at 20 °C is negligible compared to that at 50 °C. After inserting the sample in the NMR probe, a coarse optimization of the Z1–Z3 shims was performed, and ^1H-^{15}N gradient-HSQC spectra (Kay et al., 1992) were acquired as a function of time. HSQC spectra were acquired with 2,048 complex points in the ^1H dimension and 100 complex points in the ^{15}N dimension. A total of 22 HSQC spectra were collected over a period of 3 h for the protein in the presence of DTT. For the oxidized protein 38 HSQC spectra were collected over a period of 18 h. Experimental dead-times were 10 min and 7 min for the oxidized and the reduced protein, respectively.

The intensity maximum of each crosspeak in the HSQC spectrum was measured as a function of exchange time, defined as the period from the insertion of the sample into the NMR probe to the end of each HSQC experiment. Rate constants for exchange were obtained from a non-linear least-squares fit of the exponential decay data to the equation (Bai et al., 1993):

$$I = I_o \exp(-k_{obs} t) + C$$

with the initial intensity I_o, the baseline C, and the observed exchange rate k_{obs} as free variables in the fit. Protection factors were

calculated from the observed exchange rates, and the intrinsic rates of Bai et al. (1993).

Acknowledgments

We thank Klara Rathgeb-Szabo for the preparation of some of the CMPcc samples, and Ariel Lustig for analytical ultracentrifugation measurements. This work supported by Swiss National Science Foundation grants 31-43091.95 to A.T.A and 31-32251.91 to J.E.

References

Alexandrescu AT, Dames SA, Wiltscheck R. 1996. A fragment of staphylococcal nuclease with an OB-fold structure shows hydrogen-exchange protection factors in the range reported for "molten globules." *Protein Sci 5*:1942–1946.

Antonsson P, Kammerer RA, Schulthess T, Hänisch G, Engel J. 1995. Stabilization of the α-helical coiled coil domain in laminin by C-terminal disulfide bonds. *J Mol Biol 250*:74–79.

Archer SJ, Ikura M, Torchia DA, Bax A. 1991. An alternative 3D NMR technique for correlating backbone ^{15}N with side chain Hβ resonances in larger proteins. *J Magn Reson 95*:636–641.

Argraves WS, Deák F, Sparks KJ, Kiss I, Goetinck PF. 1987. Structural features of cartilage matrix protein deduced form cDNA. *Proc Natl Acad Sci USA 84*:464–468.

Bai Y, Milne JS, Mayne L, Englander SW. 1993. Primary structure effects on peptide group hydrogen exchange. *Proteins 17*:75–86.

Bai Y, Sosnick TR, Mayne L, Englander SW. 1995. Protein folding intermediates: Native-state hydrogen exchange. *Science 269*:145–151.

Bax A, Pochapsky SS. 1992. Optimized recording of heteronuclear multidimensional NMR spectra using pulsed field gradients. *J Magn Reson 99*:638–643.

Beck K, Gambee JE, Bohan CA, Bächinger HP. 1996. The C-terminal domain of cartilage matrix protein assembles into a triple-stranded α-helical coiled coil structure. *J Mol Biol 256*:909–923.

Berger B, Wilson DB, Wolf E, Tonchev T, Milla M, Kim PS. 1995. Predicting coiled coils by use of pairwise residue correlations. *Proc Natl Acad Sci USA 92*:8259–8263.

Betz SF, Byson JW, DeGrado WF. 1995. Native-like and structurally characterized α-helical bundles. *Curr Opin Struct Biol 5*:457–463.

Budisa N, Steipe B, Demange P, Eckerskorn C, Kellermann J, Huber R. 1995. High-level biosynthetic substitution of methionine in proteins by its analogs 2-aminohexanoic acid, selenomethionine, telluromethionine and ethionine in *Escherichia coli*. *Eur J Biochem 230*:788–796.

Cohen C, Parry, DAD. 1990. α-Helical coiled coils and bundles: How to design an α-helical protein. *Proteins 7*:1–15.

Davis AL, Keeler J, Laue ED, Moskau D. 1992. Experiments for recording pure-absorption heteronuclear correlation spectra using pulsed field gradients. *J Magn Reson 98*:207–216.

Deák F, Piecha D, Bachratl C, Paulsson M, Kiss I. 1997. Primary structure and expression of matrilin-2, the closest relative of cartilage matrix protein within the von Willebrand factor type A module superfamily. *J Biol Chem 272*:9268–9274.

Folkers PJM, Folmer RHA, Konings RNH, Hilbers CW. 1993. Overcoming the ambiguity problem encountered in the analysis of nuclear Overhauser magnetic resonance spectra of symmetric dimer proteins. *J Am Chem Soc 115*:3798–379.

Forsén S, Hoffman RA. 1963. Study of moderately rapid chemical exchange reactions by means of nuclear magnetic double resonance. *J Chem Phys 39*:2892–2901.

Gonzalez L Jr, Woolfson DN, Alber T. 1996. Buried polar residues and structural specificity in the GCN4 leucine zipper. *Nat Struct Biol 3*:1011–1018.

Gribskov M, Devereux J, Burgess RR. 1984. The codon preference plot: Graphic analysis of protein coding sequences and prediction of gene expression. *Nucleic Acid Res 12*:539–549.

Harbury PB, Zhang T, Kim PS, Alber T. 1993. A switch between two-, three-, and four-stranded coiled coils in GCN4 leucine zipper mutants. *Science 262*:1401–1407.

Harbury PB, Kim PS, Alber T. 1994. Crystal structure of an isoleucine-zipper trimer. *Nature 371*:80–83.

Haudenschild DR, Tondravi MM, Hofer U, Chen Q, Goetinck PF. 1995. The role of coiled coil α-helices and disulfide bonds in the assembly and stabilization of cartilage matrix protein subunits. A mutational analysis. *J Biol Chem 270*:23150–23154.

Hauser N, Paulsson M. 1994. Native cartilage matrix protein (CMP). A compact trimer of subunits assembled via a coiled coil α-helix. *J Biol Chem 269*:25747–25753.

Hodges RS, Sodek J, Smillie LB, Jurasek L. 1972. Tropomyosin: Amino acid sequence and coiled-coil structure. *Cold Spring Harbor Symp Quant Biol 37*:299–310.

Junius FK, O'Donoghue SI, Nilges M, Weiss AS, King GF 1996. High resolution NMR structure of the leucine zipper domain of the c-Jun homodimer. *J Biol Chem 271*:13663–13667.

Kammerer RA, Antonsson P, Schulthess T, Fauser C, Engel J. 1995. Selective chain recognition in the C-terminal α-helical coiled coil region of laminin. *J Mol Biol 250*:64–73.

Kammerer RA. 1997. α-Helical coiled coil oligomerization domains in extracellular proteins. *Matrix Biol 15*:555–565.

Kay LE, Clore GM, Bax A, Gronenborn AM 1990. Four-dimensional heteronuclear triple-resonance NMR spectroscopy of interleukin-1β in solution. *Science 249*:411–414.

Kay LE, Keifer P, Saarinen T. 1992. Pure absorption gradient enhanced heteronuclear single quantum correlation spectroscopy with improved sensitivity. *J Am Chem Soc 114*:10663–10665.

Kay LE. 1995. Pulsed field gradient multi-dimensional NMR methods for the study of protein structure and dynamics in solution. *Prog Biophys Mol Biol 63*:277–299.

Lee W, Revington MJ, Arrowsmith C, Kay LE. 1994. A pulsed field gradient isotope-filtered 3D ^{13}C HMQC-NOESY experiment for extracting intermolecular NOE contacts in molecular complexes. *FEBS Lett 350*:87–90.

Lupas A. 1996. Coiled coils: New structures and new functions. *Trends Biochem Sci 21*:375–382.

Lupas A, van Dyke M, Stock J. 1991. Predicting coiled coils from protein sequences. *Science 252*:1162–1164.

Malashkevich VN, Kammerer RA, Efimov VP, Schulthess T, Engel J. 1996. The crystal structure of a five-stranded coiled coil in COMP: A prototype ion channel? *Science 274*:761–765.

Marion D, Ikura M, Tschudin R, Bax A. 1989. Rapid recording of 2D NMR spectra without phase cycling. Application to the study of hydrogen exchange in proteins. *J Magn Reson 85*:393–399.

McLachlan AD, Stewart M. 1975. Tropomyosin coiled-coil interactions: Evidence for an unstaggered structure. *J Mol Biol 98*:293–304.

McCoy M, Mueller L. 1992. Selective shaped pulse decoupling in NMR: Homonuclear [^{13}C] carbonyl decoupling. *J Am Chem Soc 114*:2108–2112.

Neri D, Szyperski T, Otting G, Senn H, Wüthrich K. 1989. Stereospecific nuclear magnetic resonance assignments of the methyl groups of valine and leucine in the DNA-binding domain of the 434 repressor by biosynthetically directed fractional ^{13}C labeling. *Biochemistry 28*:7510–7516.

O'Donoghue SI, Junius FK, King GF. 1993. Determination of the structure of symmetric coiled coil proteins from NMR data: Application of the leucine zipper proteins Jun and GCN4. *Protein Eng 6*:557–564.

Parry DAD. 1982. Coiled-coils in α-helix containing proteins: Analysis of the residue types within the heptad repeat and the use of these data in the prediction of coiled coils in other proteins. *Biosci Rep 2*:1017–1024.

Paulsson M, Heinegård D. 1981. Purification and structural characterization of a cartilage matrix protein. *Biochem J 197*:539–545.

Richardson JS, Richardson DC. 1988. Amino acid preferences for specific locations at the ends of α helices. *Science 240*:1648–1652.

Schägger H, von Jagow G. 1987. Tricine-sodium dodecyl sulfate-polyacrylamide gel electrophoresis for the separation of proteins in the range from 1 to 100 kDa. *Anal Biochem 166*:368–379.

Shaka AJ, Keeler J, Freeman R. 1983. Evaluation of a new broadband decoupling sequence: WALTZ-16. *J Magn Reson 53*:313–340.

Shaka AJ, Barker PB, Freeman R. 1985. Computer-optimized decoupling scheme for wideband applications and low-level operation. *J Magn Reson 64*:547–552.

Shaka AJ, Lee CJ, Pines A. 1988. Iterative schemes for bilinear operators: Application to spin decoupling. *J Magn Reson 77*:247–293.

Shoemaker DP, Garland CW, Steinfeld JI, Nibler JW. 1981. *Experiments in physical chemistry*. New York: McGraw-Hill.

Studier FW, Rosenberg AH, Dunn JJ, Dubendorf JW. 1990. Use of T7 RNA polymerase to direct the expression of cloned genes. *Methods Enzymol 185*:60–89.

Tondravi MM, Winterbottom N, Haudenschild DR, Goetinck PF. 1993. Cartilage matrix protein binds to collagen and plays a role in collagen fibrillogenesis. *Prog Clin Biol Res 383B*:512–522.

van Holde KE. 1985. *Physical biochemistry*. Engelwood Cliffs, NJ: Prentice Hall. pp 110–129.

Vuister GW, Bax A. 1993. Quantitative *J* correlation: A new approach for

measuring $J(H^N H^\alpha)$ coupling constants in ^{15}N-enriched proteins. *J Am Chem Soc 115*:7772–7777.

Winterbottom N, Tondravi MM, Harrington TL, Klier FG, Vertel BM, Goetinck PF. 1992. Cartilage matrix protein is a component of the collagen fibril of cartilage. *Dev Dynam 193*:266–276

Wishart DS, Sykes BD, Richards FM. 1991. Relationship between nuclear magnetic resonance chemical shifts and protein secondary structure. *J Mol Biol 222*:311–333.

Wishart DS, Bigam CG, Holm A, Hodges RS, Sykes BD. 1995a. ^1H, ^{13}C, and ^{15}N random coil chemical shifts of the common amino acids. I. Investigation of nearest-neighbor effects. *J Biomol NMR 5*:67–81.

Wishart DS, Bigam CG, Yao J, Abildgaard F, Dyson HJ, Oldfield E, Markley JL, Sykes BD. 1995b. ^1H, ^{13}C and ^{15}N chemical shift referencing in biomolecular NMR. *J Biomol NMR 6*:135–140.

Woolfson DN, Alber T. 1995. Predicting oligomerization states of coiled coils. *Protein Sci 4*:1596–1607.